Journal of Power Sources 269 (2014) 550–555

Contents lists available at ScienceDirect

Journal of Power Sources

journal homepage: www.elsevier.com/locate/jpowsour

Synthesis of copper sulfide nanowire bundles in a mixed solvent as a cathode material for lithium-ion batteries

Caihong Feng [a, b], Le Zhang [a], Zhihui Wang [b], Xiangyun Song [b], Kening Sun [a], Feng Wu [a], Gao Liu [b, *]

[a] School of Chemical Engineering and Environment, Beijing Institute of Technology, Beijing 100081, PR China
[b] Lawrence Berkeley National Laboratory, 1 Cyclotron Rd., MS 70R108B, Berkeley, CA 94720, USA

HIGHLIGHTS

- Novel copper sulfide (CuS) nanowire bundles were successfully synthesized.
- A template- and surfactant-free method in a dimethyl sulfoxide (DMSO)-ethyl glycol (EG) mixed solvent was used.
- The synthesized material exhibit a large capacity and excellent cycling stability and rate capability.
- The unique structure of the CuS nanowire bundles is responsible for their excellent electrochemical performance.

ARTICLE INFO

Article history:
Received 28 April 2014
Received in revised form
27 June 2014
Accepted 1 July 2014
Available online 9 July 2014

Keywords:
Copper sulfide
Nanowire bundles
Mixed solvent
Lithium-ion batteries

ABSTRACT

Novel copper sulfide (CuS) nanowire bundles with a diameter of about 6 nm and a length up to several micrometers are successfully synthesized by a template- and surfactant-free method in a dimethyl sulfoxide (DMSO)-ethyl glycol (EG) mixed solvent. The resulting CuS nanowire bundles are used as a cathode material in lithium-ion batteries and exhibit a large capacity and excellent cycling stability and rate capability. The unique structure of the CuS nanowire bundles is responsible for their excellent electrochemical performance.

1. Introduction

The increasing demand of renewable energy sources continues to inspire an enormous amount of research interest in new electrode materials and electrode materials with new structures for lithium- ion batteries (LIBs). Recent progress has demonstrated that the performance of LIBs not only strongly relies on the electrode materials used but also on the morphology and the microstructure of the electrode materials used [1,2]. Up to now, significantly improved battery performance of various nanoscale materials—including transition metal oxide nanoparticles [3,4], Cu–Si nanocables [5,6], and metal chalcogenides [7,8]—has been reported. The outstanding electrochemical performance is ascribed to the new nanostructure, which can increase reaction sites, improve cycle life in the face of mechanical strain, and improve efficient charge transport.

Copper sulfides have received considerable attention due to their wide stoichiometric composition (Cu_xS, $x = 1–2$) and diverse applications in energy devices [9,10]. Among them, green covellite copper sulfide (CuS) has been actively investigated as an electrode material for LIBs due to its cost effectiveness, abundance in nature, environmental friendliness, good electronic conductivity (10^3 S^{-1}) and higher theoretical lithium-ion (Li-ion) storage capacity (560 mA h g^{-1}) than that of commonly used cathode material $LiCoO_2$ (145 mA h g^{-1}) [11–13]. Although CuS is known to suffer from poor capacity retention, and hence a short lifetime, much enhanced electrochemical performance can be expected by nanostructuring CuS or by using an ether-based electrolyte [14,15]. In the past few years, many attempts have focused on the synthesis of novel nanostructures of copper sulfides, including hollow

* Corresponding author. Tel.: +1 510 486 7207; fax: +1 510 486 7303.
E-mail address: gliu@lbl.gov (G. Liu).

http://dx.doi.org/10.1016/j.jpowsour.2014.07.006
0378-7753/

spheres and flowers [16–18], one-dimensional (1-D) nanostructures [19–22], and complex hierarchical micro-/nanostructures [23–28]. Among different kinds of nanoscale morphologies, 1-D nanostructures attract wide interest because of their advantages in electronic conduction along the axial direction. The corresponding preparation techniques involved mostly template-based, surfactant-directed, or interface methods. These growth methods usually require the use of special instruments, surfactants, or templates, which will increase the difficulty of operation, the cost, and contamination. A simple method for the large-scale synthesis of CuS nanowire bundles has not been achieved so far. Recent studies have shown that the mixed solvent method is effective in preparing metal chalcogenides with unique morphologies or new nanostructures because of the "magic power" of mixed solvents for shaping nanocrystals [29,30]. The solvent plays an important role in controlling the growth of nanocrystals because of its strong coordination with metal ion or selective binding with crystal plane [28,31,32]. By changing the components and volume rations of mixed solvents, it is easy to control the size, morphology, and microstructure of the desired materials. For example, urchin-like nickel selenium (NiSe) was synthesized in a ternary solution of diethylenetriamine, hydrazine hydrate, and water by S. Yu and co-workers [30]. The surface topography of these NiSe nanocrystals can be tailored by tuning the composition of the solvents used.

In this work, we report a template- and surfactant-free method for synthesizing CuS nanowire bundles in a dimethyl sulfoxide (DMSO)-ethyl glycol (EG) mixed solvent, which could be scaled up to prepare large amounts of oriented attachment CuS nanowire bundles. The factors influencing formation of CuS nanowire bundles were discussed and the electrochemical properties of as-prepared CuS cathode were investigated as well. The unique structure of CuS nanowire bundles offers many critical features, such as a fast way for both ion and electron transport, many active sites for electrode reactions, and a robust structure for durability [33], which make it a promising cathode material for LIBs with high capacity, excellent rate performance, and high cycling stability.

2. Experimental

2.1. Materials

Thiourea (ACS reagent, 99.0%), copper (II) nitrate trihydrate ($Cu(NO_3)_2 \bullet 3H_2O$), ethylene glycol (EG, anhydrous, 99.8%), and dimethyl sulfoxide (DMSO, GC, 99.5%) were purchased from Sigma–Aldrich. Lithium-ion electrolytes were purchased from Novolyte Technologies, including 1 M lithium hexafluorophosphate ($LiPF_6$) in ethylene carbonate (EC) and diethyl carbonate (DEC) (1:1 w/w) with 30% fluoroethylene carbonate (FEC). All chemicals were used without further purification.

2.2. Synthesis of the CuS nanowires bundles

In a typical synthesis, 0.290 g of $Cu(NO_3)_2 \bullet 3H_2O$ was dissolved in the mixed solvent (60 mL) with a volume ratio of V_{DMSO}/V_{EG} (defined as R) = 1:3 under stirring in a three-neck flask at room temperature. The temperature of the solution was slowly increased to 145 °C and was maintained for 3 h under nitrogen ambience. Then, 5 ml of mixed solution containing 0.274 g of thiourea was added to the solution drop by drop through a syringe under vigorous stirring. Finally, the whole solution was kept at 160 °C for another 2 h. The final products were collected by centrifugation and washed several times by distilled water and ethanol and dried in a vacuum at 60 °C for 12 h.

2.3. Material characterization

The phase composition of the as-prepared samples were characterized by a Philips X'Pert Pro Multipurpose X-ray diffractometer (XRD) using Cu Kα radiation at 45 kV and 40 milliamps (mA), at the 2θ range 20°–85° with 0.02 per step. The Raman spectra of the sample were collected using a Renishaw spectrophotometer equipped with a microscope having a laser wavelength of 532 nm. The morphology of the samples and electrodes was characterized with a JEOL JSM-7500F field emission scanning electron microscope (SEM) system. High-resolution transmission electron microscope (TEM) images were obtained on a Philips CM200 field emission microscope operated at 200 kV.

2.4. Electrochemical measurement

The as-prepared CuS nanowire bundles were studied as cathode materials for rechargeable lithium-ion batteries. The anodes were fabricated by mixing copper sulfur nanowires, Super C 65, carboxymethyl cellulose (CMC), and Polyvinyl Alcohol (PVA) with a weight ratio of 75:15:7.5:2.5 in water. The mixture was blended together using a Polytron PT 10–35 homogenizer at 2500 rpm for

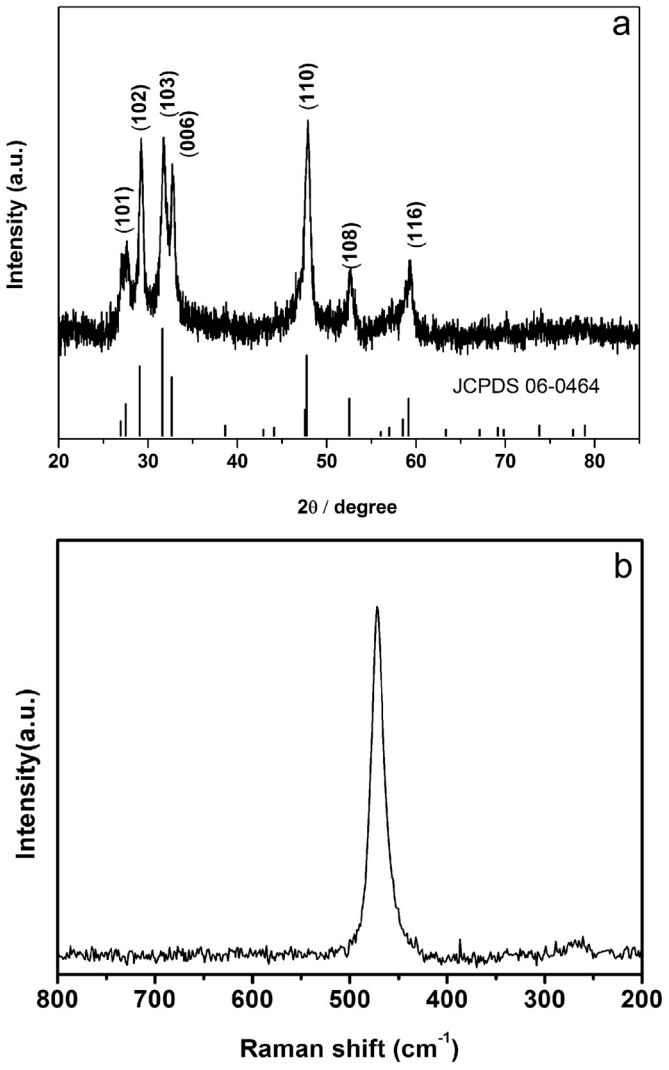

Fig. 1. (a) XRD patterns of as-grown CuS nanowire bundles; (b) Raman spectra of as-grown CuS nanowire bundles.

40 min. The slurries were coated on copper foil with a doctor-blade and dried at room temperature. The circular electrodes were punched out and were further dried under vacuum at 100 °C for 16 h before being assembled. The coin-type cells were assembled in an argon-filled glove box (H_2O, O_2 < 1 ppm). Electrochemical measurements were carried out on CR2325 coin cell hardware with Li counter electrodes and Celgard 2400 separators at different current rates (0.1C, 0.2C, 0.5C, 1C, and 2C; 1C = 560 mA g^{-1}). The electrolyte solution was made of 1 M $LiPF_6$ in EC/DEC (1:1 w/w) with 30% FEC. The cyclic voltammetry (CV) was performed in a three-electrode cell with lithium foil as a counter and reference electrodes, by using an electrochemical workstation at room temperature. The CV tests were carried out at a potential scan rate of 0.02 mV per second (mV s^{-1}) between 0.05 and 2.7 V.

3. Results and discussion

3.1. Crystal structure and morphology

The structures of the as-grown CuS nanowire bundles were determined by X-ray diffraction (XRD). The XRD pattern of the as-prepared product is shown in Fig. 1. All the diffraction peaks can be indexed to the hexagonal phase of CuS (JCPDS No. 06 0464), and no impurity phases can be detected, indicating the formation of pure CuS and that they are highly crystalline. The broadening of the diffraction peaks also indicates that the products have small sizes. Raman spectroscopy was employed to further characterize the overall symmetry of the as-prepared CuS nanowire bundles, as shown in Fig 1(b). A strong, sharp band at 475 cm^{-1} was dominant in the spectrum and has been previously associated with S–S stretching vibrational mode of the covellite system [34].

The morphology and size of the as-prepared products has been studied by SEM and is shown in Fig. 2. The SEM images not only reveal that the product is composed of nanowires with a uniform diameter of about 6 nm and lengths up to several micrometers, but also show that nanowire bundles of high yield and good uniformity can be easily achieved with this simple and easily controlled approach. More details of the nanowires are revealed in the high magnification image. As shown in Fig. 2(b), the nanowires have rough surfaces and some particles are attached to them. What is more interesting is that most of these nanowires self-assemble into bundles of nanowires.

To study the growth direction and microstructure of the bundles of nanowires, the product was further investigated by TEM and HRTEM. As shown in Fig. 3(a) and (b), nanowires array side-by-side and self-assemble into the bundles. The high-resolution TEM image (Fig. 3(b)) shows the lattice fringes, and both of the fringe spaces were determined to be 0.28 nm, which can be indexed as the (103)

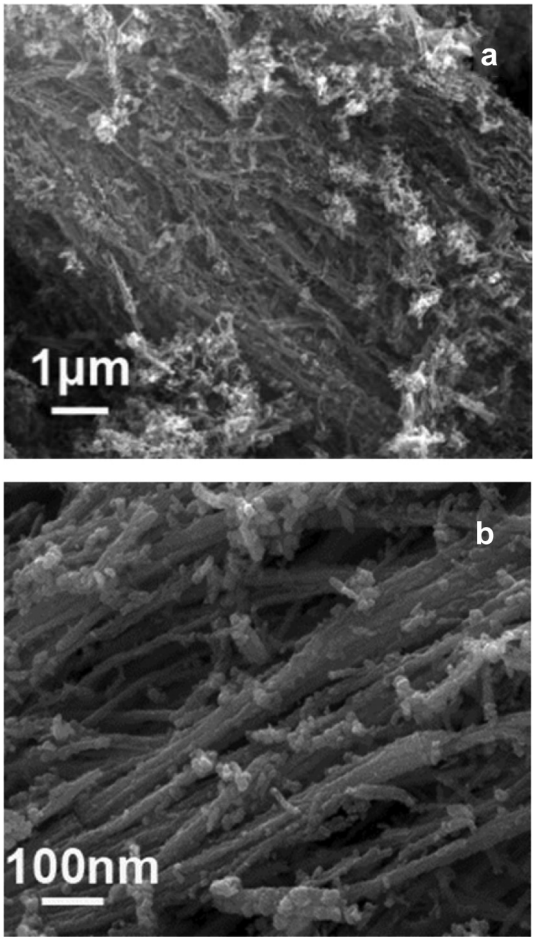

Fig. 2. (a) Low-magnification view of a large-area of CuS nanowire bundles. (b) High-magnification view of self-assembled CuS nanowire bundles.

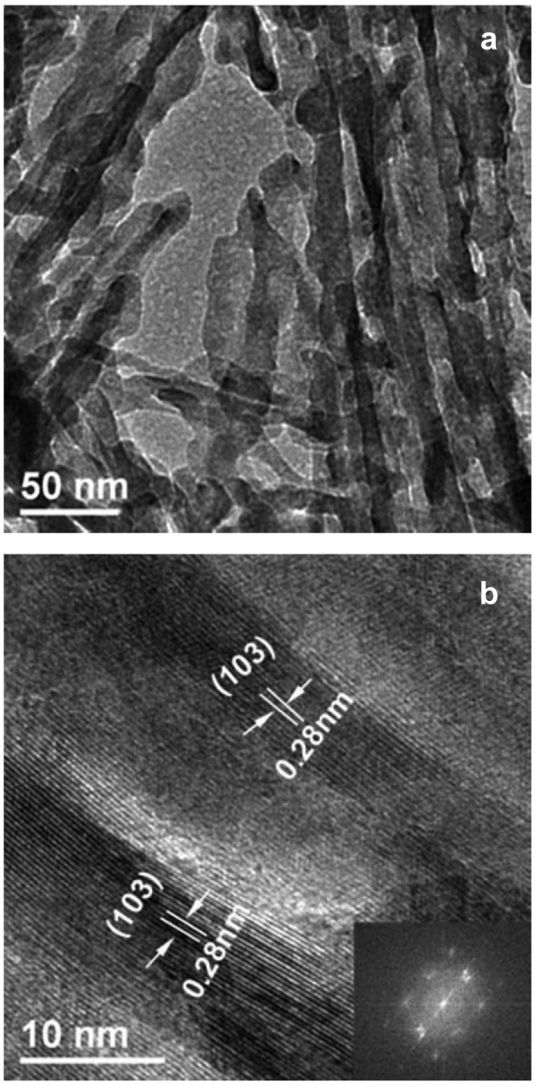

Fig. 3. (a) Low-magnification TEM image of oriented CuS nanowire bundles. (b) High-resolution TEM images of oriented CuS nanowire arrays. The inset in (b) is the corresponding selected area electron diffraction (SAED) patterns of CuS.

planes of CuS. It also clearly reveals the orientations of the atomic lattice fringes are almost parallel to each other. This indicates that the CuS prefer to orient themselves with similar crystallographic facets. The corresponding selected area electron further confirms the same growth direction of these wires.

It has been proved that the mixed solvent has key effects and often serves as the structure-directing coordination (template effect) in the controlling formation of nanostructures [35]. Y. Du has reported that the composition of solvents has a great effect on the morphology of CuS nanosheet formation [14]. J. Kundu has controlled synthesis CuS nanostructured assemblies with different morphologies by varying the solvent [36]. In our case, controlled experiments were performed to understand the effluence of the mixed solvent on the formation of CuS nanowire bundles. We changed the ratio of mixed solvent gradually and keep other conditions constantly. Fig. 4(a)–(e) shows the SEM images of CuS samples collected in mixed solvent with a different volume ratio. In the DMSO medium, the as-prepared products mainly consisted of a hexagonal plate stack with a diameter about 2–3 micrometers (μm) (Fig. 4(a)). In the EG medium, the products were fluffy hierarchical nanostructures (Fig. 4(e)). These hierarchical nanostructures consist of nanoplates with a width of about 100 nm. When mixed solvent of EG and DMSO was used as solvent instead of simplex solvent, the morphology changed with the varying solvent. As shown in Fig. 4(b)–(d), we can obtain the CuS nanowire only when the ratio of DMSO in the mixed solvent is lower than 3:7. Otherwise, the products proved to be irregular particles. This may be caused by the special chemical and physical properties of EG and DMSO [37]. Just by changing the ratio of the solvent, we can control the final shape of the CuS, which avoids complicated processes and special instruments and is convenient for preparing nanowires.

3.2. Electrochemical performance

The layered crystallographic feature of CuS allows for the intercalation and reaction of Li^+ in between the S–Cu–S layers [14], making the CuS nanowires arrays a promising electrode material for Li-ion battery applications. Fig. 5(a) shows the charge–discharge voltage profiles of the CuS electrode for the first,

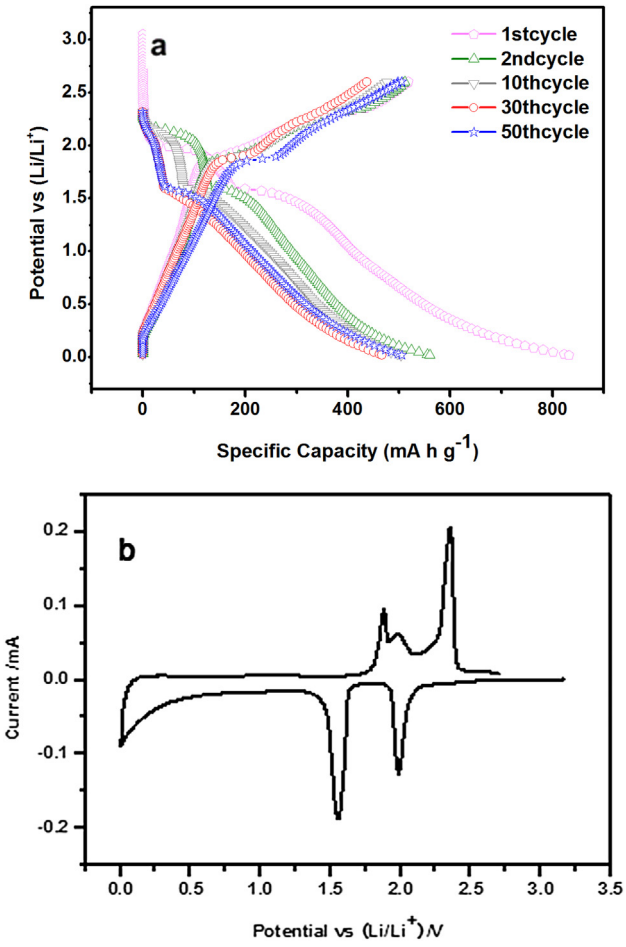

Fig. 5. The charge–discharge curves of (a) the prepared CuS cathode at 0.2C rate during cycling, and (b) CV curves of the CuS cathode in the first cycle. The potential scanning rate is 0.02 mV s^{-1} between 0.02 and 2.7 V.

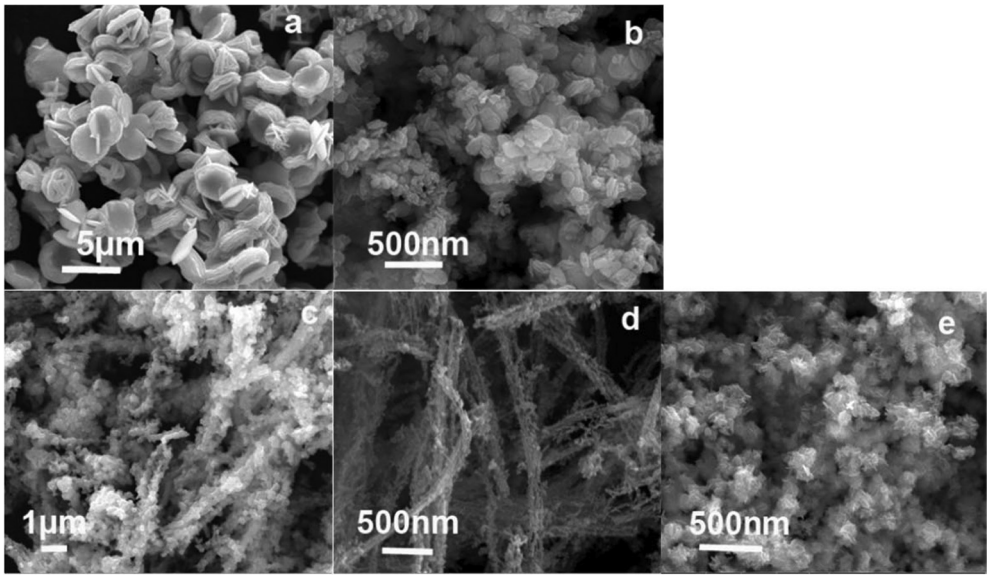

Fig. 4. SEM images of as-prepared CuS nanostructures obtained from different solvents as other conditions were kept constant: (a) DMSO as solvent; (b) 3:1 DMSO-EG as solvent; (c) 3:7 DMSO-EG as solvent; (d) 1:4 DMSO-EG as solvent; (e) EG as solvent.

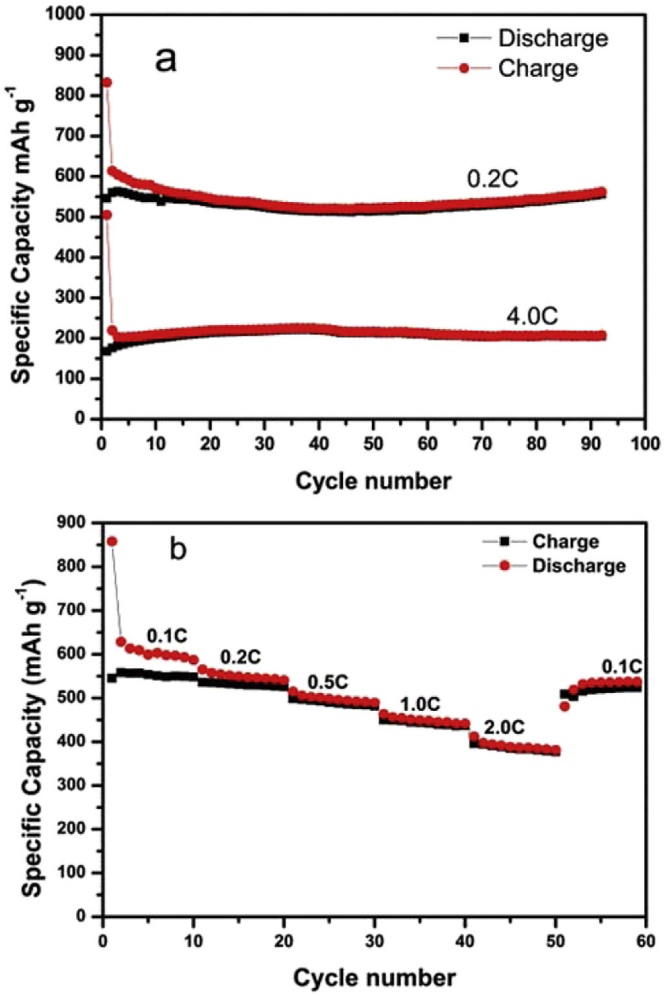

Fig. 6. (a) The cycling performance of the CuS cathode at 0.2C and 4C; (b) Cycling stability at various C-rates for CuS nanowire bundles.

second, tenth, thirtieth, and fiftieth cycle at a constant current rate of 0.2C. The electrode displays an initial discharge capacity of 831 milliamp hours per gram (mA h g^{-1}) and a charge capacity of 518 mA h g^{-1}. The initial higher-than-theoretical capacity should be largely attributed to the formation of solid electrolyte interface (SEI) film or gel-like polymeric layers and is also previously observed in CuS nanospheres and other systems of metal chalcogenide cathode materials operating through Li^+ insertion/extraction reactions [38,39]. Subsequently, the discharge capacity decreases to 560, 505, and 470 mA h g^{-1} at the second, the tenth and the thirtieth cycle, respectively, then increases to 505 mA h g^{-1} at the fiftieth cycle.

The voltage profile shows that the reaction process consists of two main steps. During the first discharge process, voltage drops from the open circuit voltage (OCV) to 2.2 V and reaches a plateau at 2.09 V. A second plateau occurs at about 1.60 V, followed by a long slope until cutoff voltage (0.02 V). According to literature [8,12,13,18], the two- step reactions can be described as shown below:

First discharge plateau reaction:

$$CuS + xLi^+ + xe^- \rightarrow Li_xCuS \quad (1)$$

Second discharge plateau reaction:

$$Li_xCuS + Li^+ + e^- \rightarrow Li_2S + Cu \quad (2)$$

It can be seen from Fig. 5(a) that the plateau at 2.09 V becomes shorter and the voltage plateau region becomes higher during the discharge process, and no distinct plateau potential regions can be observed near 2.09 V after 10 cycles. Accordingly, the plateau at 1.60 V becomes longer, and the voltage plateau region becomes lower during the charge process, which means that the electrochemical reactions change gradually and the reversibility of the CuS cathode improves with cycling [12,15].

The CV measurements were also preformed to characterize the electrochemical reaction of the CuS electrode in the first cycle. As shown in Fig. 5(b), two reduction peaks appear at about 2.0 V and 1.6 V, and two oxidation peaks are present at 1.9 V and 2.4 V, which coincides with the discharge–charge curves in Fig. 5(a).

Fig. 6(a) depicts the cycling performance of the CuS cathode at a 0.2C rate and a 4C rate. As shown in Fig. 6(a), the electrode of CuS exhibits a discharge-specific capacity of 832 mA h g^{-1} and a charge capacity of 518 mA h g^{-1} at the first cycle. After 30 cycles, the capacity becomes stable, and a coulombic efficiency of 98.8% can be obtained. When the current density is increased 20 times, from 0.2C to 4.0C, a charge capacity of 196 mA h g^{-1} and coulombic efficiency of 99.0% are achieved, demonstrating a higher lithium storage capability, an excellent cycling stability, and a good capacity retention of the electrode than previous reported [12,13,17,25].

In addition to high capacity and good capacity stability, the CuS cathode exhibits a very good rate capability (Fig. 6(b)). Under the condition of 0.1C discharge current between 0.02 V and 2.6 V, the CuS electrode shows a reversible capacity of 548 mA h g^{-1} after the tenth cycle and shows columbic efficiency of 92%. The capacity decreases gradually while the discharge current density increases. The reversible capacity of CuS electrodes at other various rates are

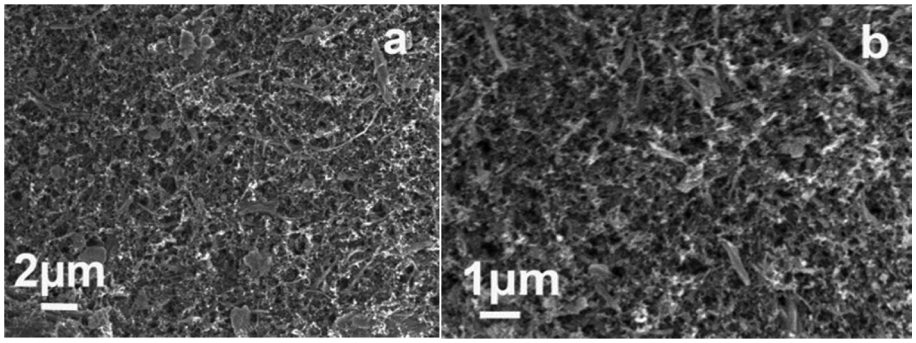

Fig. 7. (a) SEM image of the CuS electrode before discharge/charge cycles. (b) SEM image of the CuS electrode after 40 discharge/charge cycles.

510 mA h g^{-1}, 482 mA h g^{-1}, 437 mA h g^{-1}, and 377 mA h g^{-1} at 0.2C, 0.5C, 1.0C, and 2.0C, respectively, after a continuous rate change. Moreover, when the rate returns to the initial 0.1C after 50 cycles, the CuS electrode recovers its capacity to 524 mA h g^{-1}. In particular, the coulombic efficiency also increases from 93.3% for the tenth cycle at 0.1C to 96.3%, 98.5%, 98.8%, and 99.0% at the end of each cycle of a different high rate.

The long cycle life and good high-rate rate performance was proposed to be related to the advantages of the one-dimensional nanostructured electrode and direct growth of CuS nanowire bundles. To study the structural change of CuS upon cycling, the active material of the fresh CuS electrode and discharged electrodes were collected and examined by XRD (see Supporting information). Though the signal-to-noise ratio of XRD pattern is low due to the small quantity of active material, the results still clearly show that the appearance of Li_2S and metallic copper after discharge, which is consistent with the previous studies on CuS and Cu_2S [8,12,13,18]. The CuS nanowire electrode was washed gradually with dimethyl carbonate in an argon-filled glove box after 40 discharge/charge cycles and characterized by SEM. It can be seen from Fig. 7(a) and (b) that the CuS nanowires are highly dispersed in the electrode before-and-after cycles. No obvious structure destruction can be observed in the electrode after 40 discharge/charge cycles. Based on the experiments result, the 1-D nanostructures appears to provide effective accommodation of the strain during Li^+ insertion/extraction and prevents electrode degradation during the repeated charging and discharging [40]. Besides, the 1-D nanowires may shorten the transport length and enhance the transport of electrons, ions, and molecules associated with cycling of batteries, significantly accelerating the rate of chemical and energy transformation processes and leading to enhanced energy storage process [41].

4. Conclusions

In summary, we have developed a template- and surfactant-free method to fabricate CuS nanowire bundles in an EG-DMSO mixture solvent. The ratio of mixed solvent has proven to have great effect on the morphology of the bundles. The as-prepared CuS nanowire bundle cathode has shown good electrochemical performance for LIBs. The ordered assemble structure of CuS nanowire bundles is responsible for the excellent electrochemical performance, including the highly reversible capacity, excellent cyclic performance, and high coulombic efficiency with good rate capability.

Acknowledgments

This work was funded by the Assistant Secretary for Energy Efficiency, Vehicle Technologies Office of the U.S. Department of Energy, under the Batteries for Advanced Transportation Technologies (BATT) under contract no. DE-AC02-05CH11231. The State Scholarship Fund of China was organized by China Scholarship Council (CSC) and the Creative Technology Project of the Beijing Institute of Technology (No. 20131042005).

Appendix A. Supplementary data

Supplementary data related to this article can be found at http://dx.doi.org/10.1016/j.jpowsour.2014.07.006.

References

[1] M. Song, S. Park, F.M. Alamgir, J. Cho, M. Liu, Mater. Sci. Eng. R. 72 (2011) 203–252.
[2] P. Balaya, Energy Environ. Sci. 1 (2008) 645–654.
[3] N. Du, H. Zhang, J. Chen, J. Sun, B. Chen, D. Yang, J. Phys. Chem. B 112 (2008) 14836–14842.
[4] Z. Wu, W. Ren, L. Wei, L. Gao, J. Zhao, Z. Chen, G. Zhou, F. Li, H. Cheng, ACS Nano. 4 (2010) 3187–3194.
[5] F. Cao, J. Deng, S. Xin, H. Ji, O.G. Schmidt, L. Wan, Y. Guo, Adv. Mater. 23 (2011) 4415–4420.
[6] J. Qu, H. Li, J. Jr., S. Martha, N. Dudeney, H. Xu, M. Chi, M. Lance, S. Mahurin, T. Besmann, S. Dai, J. Power Sources 198 (2012) 312–317.
[7] K. Kalyanikutty, M. Nikhila, U. Maitra, C. Rao, Chem. Phys. Lett. 432 (2006) 190–194.
[8] Dupont, R. Patrice, J. Tarascon, Solid State Sci. 8 (2006) 640–651.
[9] M. Gao, Y. Xu, J. Jiang, S. Yu, Chem. Soc. Rev. 42 (2013) 2986–3071.
[10] Y. Zhao, C. Burda, Energy Environ. Sci. 5 (2012) 5564–5576.
[11] F. Bonino, M. Lazzari, B. Rivolta, B. Scrosati, J. Electrochem. Soc. 131 (1984) 1498–1502.
[12] Y. Wang, X. Zhang, P. Chen, H. Liao, S. Cheng, Electrochimica. Acta 80 (2012) 264–268.
[13] J. Chung, H. Sohn, J. Power Sources 108 (2002) 226–231.
[14] Y. Du, Z. Yin, J. Zhu, X. Huang, X. Wu, Z. Zeng, Q. Yan, H. Zhang, Nat. Commun. 3 (2012) 1177.
[15] B. Jache, B. Mogwitz, F. Klein, P. Adelhelm, J. Power Sources 247 (2014) 703–711.
[16] J. Gao, Q. Li, H. Zhao, L. Li, C. Liu, Q. Gong, L. Qi, Chem. Mater. 20 (2008) 6263–6269.
[17] Li Zhao, F. Tao, Z. Quan, X. Zhou, Y. Yuan, J. Hu, Mater. Lett. 68 (2012) 28–31.
[18] M. Nagarathinam, K. Saravanan, W. Leong, P. Balaya, J. Vittal, Cryst. Growth Des. 9 (2009) 4461–4470.
[19] C. Wu, J. Shi, C. Chen, Y. Chen, Y. Lin, P. Wu, S. Wei, Mater. Lett. 62 (2008) 1074–1077.
[20] P. Roy, K. Mondal, S. Srivastava, Cryst. Growth. Des. 8 (2008) 1530–1534.
[21] R. Cai, J. Chen, J. Zhu, C. Xu, W. Zhang, C. Zhang, W. Shi, H. Tan, D. Yang, H. Hng, T. Lim, Q. Yan, J. Phy. Chem. C. 116 (2012) 12468–12474.
[22] C. Wu, S. Yu, S. Chen, G. Liu, B. Liu, J. Mater. Chem. 16 (2006) 3326–3331.
[23] H. Yan, W. Wang, H. Xu, J. Cryst. Growth 310 (2008) 2640–2643.
[24] C. Mu, Q. Yao, X. Qu, G. Zhou, M. Li, S. Fu, Colloids Surf. A 371 (2010) 14–21.
[25] Y. Chen, C. Davoisne, J. Tarascon, C. Guéry, J. Mater. Chem. 22 (2012) 5295–5299.
[26] Y. Han, Y. Wang, W. Gao, Y. Wang, L. Jiao, H. Yuan, S. Liu, Powder Technol. 212 (2011) 64–68.
[27] J. Kundu, D. Pradhan, New. J. Chem. 37 (2013) 1470–1478.
[28] S. Yang, H. Yao, M. Gao, S. Yu, CrystEngComm 11 (2009) 1383–1390.
[29] W.T. Yao, S.H. Y u, Adv. Funct. Mater. 18 (2008) 3357–3366.
[30] M. Gao, Z. Lin, T. Zhuang, J. Jiang, Y. Xu, Y. Zheng, S. Yu, J. Mater. Chem. 22 (2012) 13662–13668.
[31] Y. Zhou, H. Yao, Y. Wang, H. Liu, M. Gao, P. Shen, S. Yu, Chem. Eur. J. 16 (2010) 12000–12007.
[32] M. Gao, Z. Lin, J. Jiang, H. Yao, Y. Lu, Q. Gao, W. Yao, S. Yu, Chem. Eur. J. 17 (2011) 5068–5075.
[33] C. Lai, K. Huang, J. Cheng, C. Lee, B. Hwang, L. Chen, J. Mater. Chem. 20 (2010) 6638–6645.
[34] B.M. Sukarawa, M. Najdoski, I. Grozdanov, C.J. Chunnial, J. Mol. Struct. 267 (1997) 410–411.
[35] G. Zou, H. Li, Y. Zhang, K. Xiong, Y. Qian, Nanotech 17 (2006) S313–S320.
[36] J. Kundu, D. Pradhan, Appl. Mater. Interfaces 6 (2014) 1823–1834.
[37] C. Feng, R. Zhang, P. Yin, Li Li, L. Guo, Z. Shen, Nanotech 19 (2008) 305601.
[38] Q. Li, Y. Xue, Y. Zhu, Y. Qian, J. Nanosci. Nanotechnol. 13 (2013) 1265–1269.
[39] Y. Gu, Y. Xu, Y. Wang, ACS Appl. Mater. Interfaces 5 (2013) 801–806.
[40] M.Y. Son, J.H. Choi, Y.C. Kang, J. Power Sources 251 (2014) 480–487.
[41] C. Lai, K. Huang, J. Cheng, C. Lee, W. Lee, W. Lee, C. Huang, B. Hwang, L. Chen, J. Mater. Chem. 19 (2009) 7277–7283.